Chemically fueled transient geometry changes in diphenic acids

Isuru M. Jayalath, Hehe Wang, Georgia Mantel, Lasith S. Kariyawasam, and C. Scott Hartley*

Department of Chemistry & Biochemistry, Miami University, Oxford, Ohio 45056, United States

Abstract

Transient changes in molecular geometry are key to the function of many important biochemical systems. Here, we show that diphenic acids undergo out-of-equilibrium changes in dihedral angle when reacted with a carbodiimide chemical fuel. Treatment of appropriately functionalized diphenic acids with EDC (*N*-(3-dimethylaminopropyl)-*N*′-ethylcarbodiimide hydrochloride) yields the corresponding diphenic anhydrides, reducing the torsional angle about the biaryl bond by approximately 45°, regardless of substitution. In the absence of steric resistance, the reaction is well-described by a simple mechanism; the resulting kinetic parameters can be used to derive important properties of the system, such as yields and lifetimes. The reaction tolerates steric hindrance ortho to the biaryl bond, although the competing formation of (transient) byproducts complicates quantitative analysis.

Many biochemical systems operate in out-of-equilibrium states that require a continuous supply of energy to maintain function.[1,2] This "dissipative" behavior imparts properties,

such as temporal control, that cannot be achieved at thermodynamic equilibrium.[3] Out-of-equilibrium geometry changes play a vital role in this context.[4–6] For example, geometry changes are fundamental to the operation of ATP-fueled molecular motor proteins;[4,5] These changes are associated with multiple cell functions, including intracellular trafficking,[4] active transport,[6] cell division,[7] signal transduction,[8] and protein translocation.[8]

Inspired by nature's example, nonbiological out-of-equilibrium behavior driven by chemical fuels has recently attracted considerable attention.[9–11] Recent work from Boekhoven,[12,13] our group,[14,15] Das,[16,17] and others[18,19] has shown that carbodiimides, typically EDC (*N*-(3-dimethylaminopropyl)-*N*′-ethylcarbodiimide hydrochloride), are useful fuels for abiotic nonequilibrium behavior. In a typical system, aqueous carboxylic acids react with carbodiimides to form carboxylic anhydrides, which subsequently undergo hydrolysis to regenerate the original carboxylic acids.

Unlike other chemical fuels (e.g., alkylating agents[9]), carbodiimides form a transient bond between two independent components. Consequently, they can be used to form intramolecular bonds,[20] a potentially useful tool for inducing changes in geometry. Here, we demonstrate a simple system that undergoes significant changes in the twist about a single bond on treatment with a chemical fuel. Our focus is the water-soluble diphenic acids shown in Figure 1a. Anhydride bond formation was expected to lead to a substantial decrease in the dihedral angle about the biaryl axis. The system acts as a sort of molecular clamp, distinct from to other systems that undergo non-equilibrium conformational switching.[21]

Diphenic acid derivatives **DP-Ac1**–**DP-Ac3** were designed to include hexaglyme groups for water solubility and a small selection of R groups to test the ability of the chemistry to work against steric resistance. DFT geometry optimizations (B97-D3(BJ)/TZV(2d,2p), Figure 1b) show that the dihedral angle about the biaryl bond in diphenic acid (ϕ_{acid}) is nearly orthogonal, as shown in Table 1. Bridging via anhydride formation reduces the twist ($\phi_{\text{anhydride}}$), with a net change $\Delta\phi$ of 45°. Ethynyl and ethyl substituents ortho to the biaryl bond increase both ϕ_{acid} and $\phi_{\text{anhydride}}$, but the net change is predicted to be similar in all

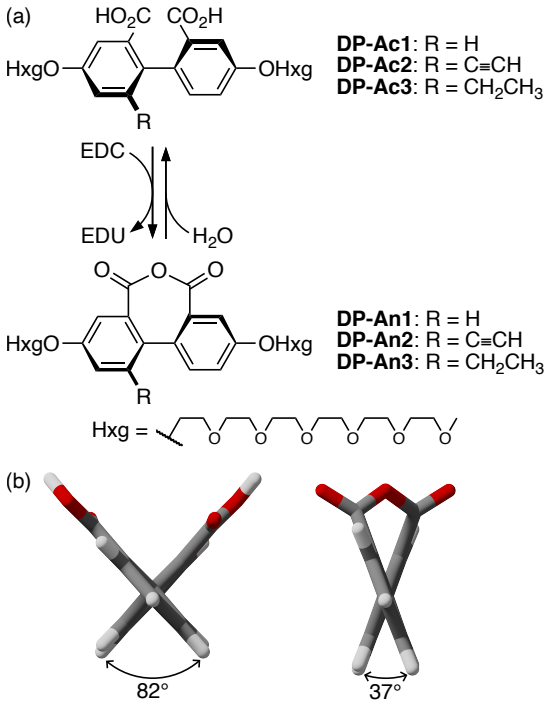

Figure 1: (a) Transient anhydride formation in the diphenic acids used in this work. (b) Model acid and anhydride geometries (R = H, OHxg removed) optimized at the B97-D3(BJ)/TZV(2d,2p) level and viewed down the biaryl axis.

three cases.

The syntheses of the target compounds began with commercially available diphenic acid **1**, as shown in Scheme 1. The synthesis of **DP-Ac1** was straightforward from compound **4** (Scheme 1a), which was synthesized following a known procedure.[22] The key intermediate for the syntheses of **DP-Ac2** and **DP-Ac3**, dimethyl 6-bromo-4,4′-dinitro-2,2′-biphenylcarboxylate **6**, was obtained from the monobromination of known[22] compound **2**

Table 1: Biaryl dihedral angles of diphenic acids and their anhydrides calculated at the B97-D3(BJ)/TZV(2d,2p) level.

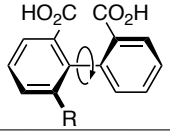

R	ϕ_{acid}	$\phi_{\text{anhydride}}$	$\Delta\phi$
H	82°	37°	45°
CCH	91°	44°	47°
CH_2CH_3	91°	50°	41°

using NBS (Scheme 1b). It was reduced, diazotized, and hydrolyzed to form intermediate **8**. Sonogashira coupling with TMS-acetylene introduced the acetyl group in **9**. This intermediate was converted to **DP-Ac2** by alkylation, giving **10** (deprotection of the TMS group occurs simultaneously), followed by saponification. This same intermediate (**10**) was subjected to catalytic hydrogenation and saponification to give **DP-Ac3**.

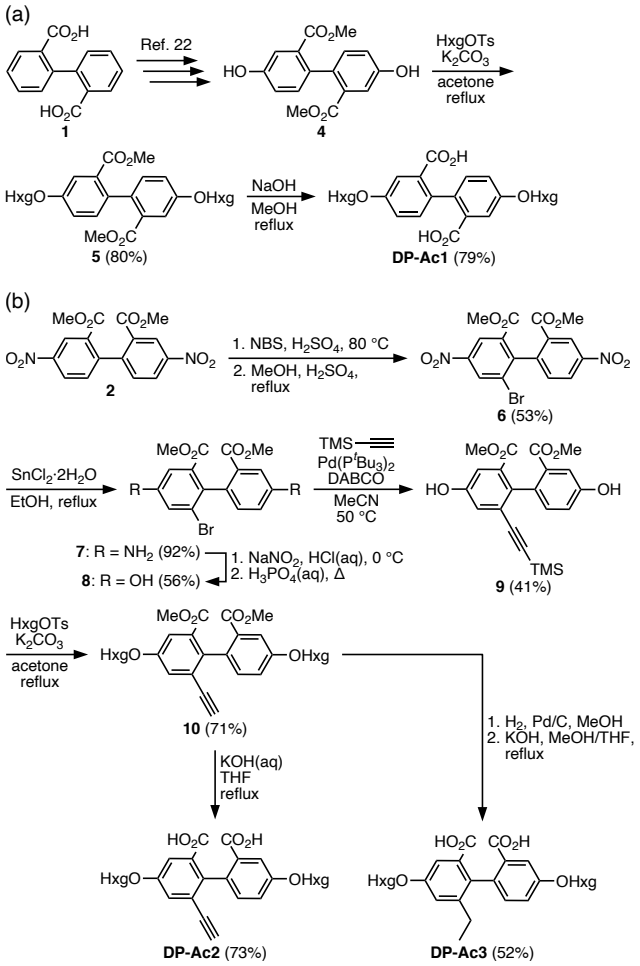

Scheme 1: Syntheses of diphenic acids (a) **DP-Ac1** and (b) **DP-Ac2**/**DP-Ac3**.

The formation of anhydride **DP-An1** from **DP-Ac1** was first monitored by in situ IR spectroscopy. Treatment of an aqueous solution of **DP-Ac1** with 0.5 equiv of EDC at 278 K resulted in the appearance of two peaks at 1775 cm^{-1} and 1738 cm^{-1} (Figure S1) which are characteristic of the symmetric and asymmetric carbonyl stretching modes of diphenic anhydrides.[23] Monitoring of the reaction in D_2O by ^1H NMR spectroscopy was also

consistent with the effective formation of the anhydride (Figures S4–S6). To further confirm that the transient species is indeed the anhydride, an authentic sample of **DP-An1** was synthesized, fully characterized, and compared with the experimental results (see Supporting Information). It is evident that formation of the intramolecular anhydride is dominant under these conditions, presumably because cyclization is favored at these relatively low concentrations and steric hindrance disfavors intermolecular coupling.

We later found water:acetone mixtures to be better solvents for **DP-Ac2** and **DP-Ac3** (see below). Accordingly, the remaining experiments for **DP-Ac1** were carried out in 7:3 D_2O:acetone-d_6 at 276 K. A typical reaction of 25 mM **DP-Ac1** with 40 mM EDC at 276 K as monitored by ^{1}H NMR spectroscopy is shown in Figure 2a. The **DP-Ac1** is rapidly consumed with the associated appearance of signals assigned to **DP-An1**. The EDC was concomitantly converted to EDU (not shown). The anhydride **DP-An1** cleanly hydrolyzes back to its parent acid **DP-Ac1** over the course of minutes. The full time course of the experiment is shown in Figure 2b.

In previous work, the addition of pyridine was necessary to avoid unproductive rearrangements of the *O*-acylisourea intermediate to the *N*-acylurea.[24,25] For the diphenic acids, no additives were necessary, as intramolecular ring closure is presumably fast enough to outcompete the rearrangement.

To better understand the mechanism, four kinetic runs were performed, varying the initial concentration of EDC ($[EDC]_0$). The data was then fit to a simple kinetic model[26–28] that describes the broad features of the system but lacks some mechanistic details, such as the pH-dependence of the rate constants and EDC speciation.[29] Initial reaction of one carboxylic acid group in diphenic acid (DA) with EDC is expected to generate an *O*-acylisourea intermediate (I) (eq 1). This intermediate can either react with the remaining acid group to form the anhydride (and EDU, eq 2), or it can undergo unproductive decomposition to reform the starting acid (and EDU, eq 3). The anhydride then hydrolyzes back to the starting acid (eq 4). A steady-state was assumed in I, which simplifies the parameters with $\alpha = k_i^{DA}/k_i^{An}$.

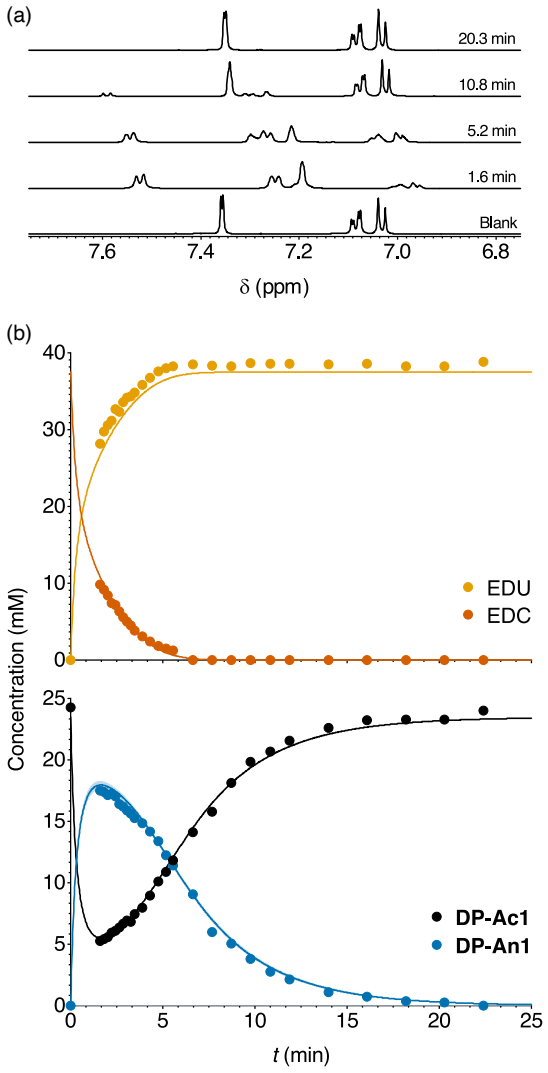

Figure 2: (a) ^{1}H NMR spectroscopy of **DP-An1** formation upon the treatment of **DP-Ac1** (25 mM) with EDC (40 mM) in D_2O:acetone-d_6 at 276 K. (b) Concentration vs time for the **DP-Ac1**/**DP-An1** system (D_2O:acetone-d_6, 7:3, 276 K) with the addition of 40 mM EDC. Solid lines represent the fits to the kinetic model and the shaded areas represent 95% confidence intervals for the fits (in some cases the CIs are narrow enough to be difficult to distinguish from the line). Note that the fits were generated by fitting to all four experiments simultaneously.

$$\mathrm{DA} + \mathrm{EDC} \xrightarrow{k_1} \mathrm{I} \tag{1}$$

$$\mathrm{I} \xrightarrow{k_i^{\mathrm{An}}} \mathrm{An} + \mathrm{EDU} \tag{2}$$

$$\mathrm{I} \xrightarrow{k_i^{\mathrm{DA}}} \mathrm{DA} + \mathrm{EDU} \tag{3}$$

$$\mathrm{An} \xrightarrow{k_2} \mathrm{DA} \tag{4}$$

The differential equations describing this mechanism were fit numerically to the complete data set for **DP-Ac1** (see Supporting Information). A representative example of the fit is shown in Figure 2b. Uncertainties (95% confidence interval) for the regression were estimated by applying a non-parametric bootstrapping method,[24] and were reasonable (shaded in Figure 2b). The resulting apparent rate constants for the **DP-Ac1** system under these conditions are $k_1 = (8.77^{+0.39}_{-0.37} \times 10^{-2})$ $\mathrm{mM}^{-1}\mathrm{min}^{-1}$, $k_2 = (2.576^{+0.069}_{-0.071} \times 10^{-1})$ min^{-1}, and $\alpha = 1.13^{+0.08}_{-0.14} \times 10^{-1}$. Confidence contour plots were generated to confirm the independence of the parameters (see Supporting Information).[30]

While these kinetic parameters fully describe the system, it can be helpful to translate them into terms that are more intuitive,[24] such as the peak anhydride concentration ($[\mathrm{An}]_{\mathrm{max}}$), the acid recovery time (τ_{99}, the time it takes for the **DP-Ac1** to return to 99% of its starting value), and the anhydride yield (the net quantity of anhydride produced relative to the amount of EDC added). For this mechanism, the yield is dependent on the partitioning of I between the anhydride (eq 2) and direct hydrolysis (eq 3), and is therefore a simple function of α (yield $= 1/(1+\alpha)$). The **DP-Ac1** system is very efficient, with a yield of 90^{+2}_{-6}%.

The peak anhydride concentration and the lifetime are both dependent on the starting concentrations of acid and carbodiimide but can be simulated from the parameters. The results of simulations of the reaction of **DP-Ac1** (25 mM) with variable amounts of starting EDC ($[\mathrm{EDC}]_0$) are shown in Figure 3. As expected, $[\mathrm{An}]_{\mathrm{max}}$ increases rapidly with increasing $[\mathrm{EDC}]_0$, approaching a limit near the starting acid concentration (Figure 3a). Because

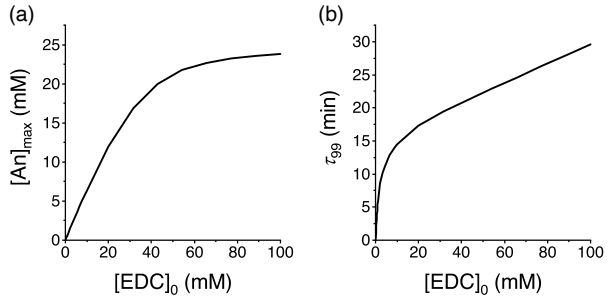

Figure 3: Simulated behavior of **DP-Ac1** (25 mM) system with variable addition of EDC. (a) Peak anhydride concentration $[An]_{max}$ vs $[EDC]_0$. (b) Time to recover 99% of the starting acid τ_{99} vs $[EDC]_0$.

hydrolysis is relatively slow compared to activation, it takes relatively little EDC to push the system to high conversion. The recovery time τ_{99} shows a sharp increase initially with increasing EDC, but then increases only slowly (Figure 3b).

We then turned to substituted derivatives **DP-Ac2** and **DP-Ac3** to determine the ability of this chemistry to act against steric resistance, which will affect its usefulness in functional systems. On treatment of both diacids with EDC, we again observe the formation of new species by ^{1}H NMR spectroscopy. These were confirmed to be the expected anhydrides **DP-An2** and **DP-An3** by comparison with independently synthesized samples (see Supporting Information). Concentration vs time data is shown in Figures 4 (and S14/S15). It is clear that the chemistry works effectively: the corresponding anhydrides form and decay as expected. The overall time scale of the reactions are longer, particularly for **DP-Ac3**. Curiously, the data obtained for **DP-Ac2** and **DP-Ac3** indicate that the hydration of EDC seems to go through two phases: faster very early on but then slowing significantly. This is possibly due to the changing pD during the reactions as the starting acids are consumed, although it is not immediately obvious why the effect is more pronounced for these systems compared to **DP-Ac1**.

Unfortunately, the NMR data for substituted derivatives failed to yield good fits to the simple mechanism described above. Even after treating with relatively large amounts of EDC, the maximum conversion peaks at about 50%, in contrast to the unsubstituted system

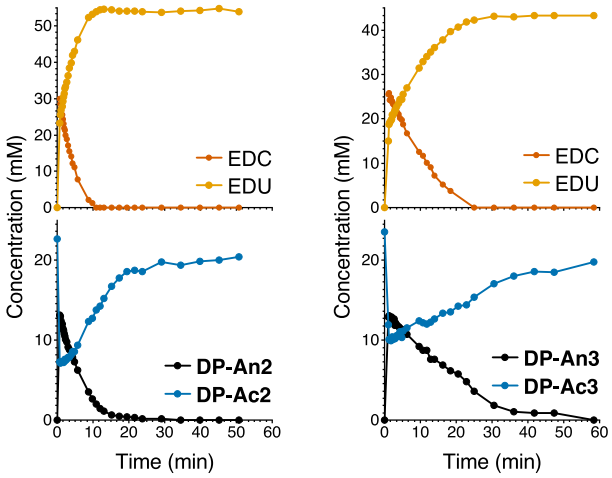

Figure 4: Representative examples of transient anhydride formation from substituted diphenic acids (D_2O:acetone-d_6, 7:3, 276 K). (a) **DP-Ac2** with the addition of 2 equiv EDC. (b) **DP-Ac3** with the addition of 2 equiv of EDC.

(compare Figures 4 and 2b). There is evidence that the formation of byproducts, likely intermolecular anhydrides, becomes significant with a higher concentrations of EDC: some broad unassigned peaks appear and disappear during the ^{1}H NMR experiments in the substituted systems (Figure S7), and it takes a longer time to fully recover the starting acids **DP-Ac2** and **DP-Ac3**. We believe that these byproducts are the result of intermolecular oligomerization, as steric hindrance in **DP-Ac2** and **DP-Ac3** disfavors cyclization. Unfortunately, these species could not be characterized or quantified. We are currently working toward experimental conditions that will yield cleaner data for these systems. Nevertheless, it is noteworthy that substantial amounts of anhydride are formed even for these more-demanding diacids, which bodes well for integrating these units within more-complex systems.

Our findings demonstrate that intramolecular anhydrides can be formed from substituted diphenic acids using EDC as a chemical fuel, leading to a transient change in the geometry of the molecule. This provides a simple platform to mimic the conformational changes observed in biological systems. More work on optimizing reaction conditions to better quantify the behavior of substituted diphenic acids, and the study of other substituted derivatives, is underway.

Acknowledgements

This work was supported by the U.S. Department of Energy, Office of Science, Basic Energy Sciences, under Award # DE-SC0018645. The purchase of the 400 MHz NMR spectrometer was supported by the National Science Foundation (CHE-1919850).

References

(1) Mattia, E.; Otto, S. Supramolecular systems chemistry. *Nat. Nanotechnol.* **2015**, *10*, 111–119.

(2) Whitesides, G. M.; Grzybowski, B. Self-assembly at all scales. *Science* **2002**, *295*, 2418–2421.

(3) van Rossum, S. A. P.; Tena-Solsona, M.; van Esch, J. H.; Eelkema, R.; Boekhoven, J. Dissipative out-of-equilibrium assembly of man-made supramolecular materials. *Chem. Soc. Rev.* **2017**, *46*, 5519–5535.

(4) Vale, R. D.; Milligan, R. A. The way things move: looking under the hood of molecular motor proteins. *Science* **2000**, *288*, 88–95.

(5) Wang, H.; Oster, G. Energy transduction in the F1 motor of ATP synthase. *Nature* **1998**, *396*, 279–282.

(6) Higgins, C. F.; Linton, K. J. The ATP switch model for ABC transporters. *Nat. Struct. Mol. Biol.* **2004**, *11*, 918–926.

(7) Roberts, A. J.; Kon, T.; Knight, P. J.; Sutoh, K.; Burgess, S. A. Functions and mechanics of dynein motor proteins. *Nat. Rev. Mol. Cell Biol.* **2013**, *14*, 713–726.

(8) Cochran, J. Kinesin motor enzymology: Chemistry, structure, and physics of nanoscale molecular machines. *Biophys. Rev.* **2015**, *7*, 269–299.

(9) Boekhoven, J.; Hendriksen, W. E.; Koper, G. J. M.; Eelkema, R.; van Esch, J. H. Transient assembly of active materials fueled by a chemical reaction. *Science* **2015**, *349*, 1075–1079.

(10) Wilson, M. R.; Solà, J.; Carlone, A.; Goldup, S. M.; Lebrasseur, N.; Leigh, D. A. An autonomous chemically fuelled small-molecule motor. *Nature* **2016**, *534*, 235–240.

(11) Rieß, B.; Grötsch, R. K.; Boekhoven, J. The design of dissipative molecular assemblies driven by chemical reaction cycles. *Chem* **2020**, *6*, 552–578.

(12) Tena-Solsona, M.; Rieß, B.; Grötsch, R. K.; Löhrer, F. C.; Wanzke, C.; Käsdorf, B.; Bausch, A. R.; Müller-Buschbaum, P.; Lieleg, O.; Boekhoven, J. Non-equilibrium dissipative supramolecular materials with a tunable lifetime. *Nat. Commun.* **2017**, *8*, 15895.

(13) Grötsch, R. K.; Wanzke, C.; Speckbacher, M.; Angı, A.; Rieger, B.; Boekhoven, J. Pathway dependence in the fuel-driven dissipative self-assembly of nanoparticles. *J. Am. Chem. Soc.* **2019**, *141*, 9872–9878.

(14) Hossain, M. M.; Atkinson, J. L.; Hartley, C. S. Dissipative assembly of macrocycles comprising multiple transient bonds. *Angew. Chem., Int. Ed.* **2020**, *59*, 13807–13813.

(15) Zhang, B.; Jayalath, I. M.; Ke, J.; Sparks, J. L.; Hartley, C. S.; Konkolewicz, D. Chemically fueled covalent crosslinking of polymer materials. *Chem. Commun.* **2019**, *55*, 2086–2089.

(16) Bal, S.; Das, K.; Ahmed, S.; Das, D. Chemically fueled dissipative self-assembly that exploits cooperative catalysis. *Angew. Chem., Int. Ed.* **2019**, *58*, 244–247.

(17) Bal, S.; Ghosh, C.; Ghosh, T.; Vijayaraghavan, R. K.; Das, D. Non-equilibrium polymerization of cross-*beta* amyloid peptides for temporal control of electronic properties. *Angew. Chem., Int. Ed.* **2020**, *59*, 13506–13510.

(18) Cheng, M.; Qian, C.; Ding, Y.; Chen, Y.; Xiao, T.; Lu, X.; Jiang, J.; Wang, L. Writable and self-erasable hydrogel based on dissipative assembly process from multiple carboxyl tetraphenylethylene derivative. *ACS Materials Lett.* **2020**, *2*, 425–429.

(19) Panja, S.; Dietrich, B.; Adams, D. J. Chemically fuelled self-regulating gel-to-gel transition. *ChemSystemsChem* **2019**, *2*, e1900038.

(20) Kariyawasam, L. S.; Hartley, C. S. Dissipative assembly of aqueous carboxylic acid anhydrides fueled by carbodiimides. *J. Am. Chem. Soc.* **2017**, *139*, 11949–11955.

(21) Jalani, K.; Dhiman, S.; Jain, A.; George, S. J. Temporal switching of an amphiphilic self-assembly by a chemical fuel-driven conformational response. *Chem. Sci.* **2017**, *8*, 6030–6036.

(22) Wang, D. H.; Cheng, S. Z.; Harris, F. W. Synthesis and characterization of aromatic polyesters containing multiple *n*-alkyl side chains. *Polymer* **2008**, *49*, 3020–3028.

(23) Kitagawa, T.; Kuroda, H.; Sasaki, H. A convenient one-pot synthesis of carboxylic acid anhydrides using 1,1'-oxalyldiimidazole. *Chem. Pharm. Bull.* **1987**, *35*, 1262–1265.

(24) Kariyawasam, L. S.; Kron, J. C.; Jiang, R.; Sommer, A. J.; Hartley, C. S. Structure–property effects in the generation of transient aqueous benzoic acid anhydrides by carbodiimide fuels. *J. Org. Chem.* **2020**, *85*, 682–690.

(25) DeTar, D. F.; Silverstein, R. Reactions of carbodiimides. I. The mechanisms of the reactions of acetic acid with dicyclohexylcarbodiimide. *J. Am. Chem. Soc.* **1966**, *88*, 1013–1019.

(26) Mironova, D. F.; Dvorko, G. F. Kinetics and mechanism of condensations involving carbodiimides. I. Solvolytic effects and mechanism of dicarboxylic acid anhydride formation in organic solvents. *Ukr. Khim. Zh. (Russ. Ed.)* **1967**, *33*, 602–614.

(27) Ibrahim, I. T.; Williams, A. Direct spectrophotometric observation of an *O*-acylisourea intermediate: concerted general acid catalysis in the reaction of acetate ion with a water-soluble carbodi-imide. *J. Chem. Soc., Perkin Trans. 2* **1982**, 1459–1466.

(28) Berliner, E.; Altschul, L. H. The hydrolysis of substituted benzoic anhydrides. *J. Am. Chem. Soc.* **1952**, *74*, 4110–4113.

(29) Ibrahim, I. T.; Williams, A. Reaction of the water-soluble reagent *N*-ethyl-*N*′-(3-dimethylaminopropyl)carbodiimide with nucleophiles: participation of the tautomeric cyclic ammonioamidine as a kinetically important intermediate. *J. Am. Chem. Soc.* **1978**, *100*, 7420–7421.

(30) Johnson, K. A.; Simpson, Z. B.; Blom, T. FitSpace Explorer: An algorithm to evaluate multidimensional parameter space in fitting kinetic data. *Anal. Biochem.* **2009**, *387*, 30–41.